Near-infrared lasers and self-frequency-doubling in Nd:YCOB cladding waveguides

Yingying Ren,[1] Feng Chen,[1,*] and Javier R. Vázquez de Aldana[2]

[1]*School of Physics, State Key Laboratory of Crystal Materials and Key Laboratory of Particle Physics and Particle Irradiation (Ministry of Education), Shandong University, Jinan 250100, China*
[2]*Laser Microprocessing Group, Universidad de Salamanca, Salamanca 37008, Spain*
[*]*drfchen@sdu.edu.cn*

Abstract: A design of cladding waveguides in Nd:YCOB nonlinear crystals is demonstrated in this work. Compact Fabry-Perot oscillation cavities are employed for waveguide laser generation at 1062 nm and self-frequency-doubling at 531 nm, under optical pump at 810 nm. The waveguide laser shows slope efficiency as high as 55% at 1062 nm. The SFD green waveguide laser emits at 531 nm with a maximum power of 100 μW.

OCIS codes: (230.7380) Waveguides, channeled; (160.3380) Laser materials; (130.3120) Integrated optics devices.

References and links

1. A. Singh, P. K. Mukhopadhyay, S. K. Sharma, K. Ranganathan, and S. M. Oak, "82 W continuous-wave green beam generation by intracavity frequency doubling of diode-side-pumped Nd:YAG Laser," IEEE J. Quantum Electron. **47**(3), 398–405 (2011).
2. V. Petrov, M. Ghotbi, O. Kokabee, A. Esteban-Martin, F. Noack, A. Gaydardzhiev, I. Nikolov, P. Tzankov, I. Buchvarov, K. Miyata, A. Majchrowski, I. V. Kityk, F. Rotermund, E. Michalski, and M. Ebrahim-Zadeh, "Femtosecond nonlinear frequency conversion based on BiB_3O_6," Laser Photon. Rev. **4**(1), 53–98 (2010).
3. N. Dong, Y. Tan, A. Benayas, J. Vázquez de Aldana, D. Jaque, C. Romero, F. Chen, and Q. Lu, "Femtosecond laser writing of multifunctional optical waveguides in a Nd:YVO_4 + KTP hybrid system," Opt. Lett. **36**(6), 975–977 (2011).
4. J. M. Eichenholz, D. A. Hammons, L. Shah, Q. Ye, R. E. Peale, M. Richardson, and B. H. T. Chai, "Diode-pumped self-frequency doubling in a Nd^{3+}:$YCa_4O(BO_3)_3$ laser," Appl. Phys. Lett. **74**(14), 1954–1956 (1999).
5. Q. Ye and B. H. T. Chai, "Crystal growth of $YCa_4O(BO_3)_3$ and its orientation," J. Cryst. Growth **197**(1-2), 228–235 (1999).
6. D. N. Nikogosyan, *Nonlinear Optical Crystals: A Complete Survey* (Springer, 2005).
7. S. F. Wang and L. F. Sang, "Diode-pumped Nd:YCOB self-frequency-doubling green laser at 530 nm," Laser Phys. **21**(8), 1347–1349 (2011).
8. C. Grivas, "Optically pumped planar waveguide lasers, Part I: Fundamentals and fabrication techniques," Prog. Quantum Electron. **35**(6), 159–239 (2011).
9. F. Chen, "Micro- and submicrometric waveguiding structures in optical crystals produced by ion beams for photonic applications," Laser Photon. Rev. **6**(5), 622–640 (2012).
10. Y. S. Kivshar, "Nonlinear optics: The next decade," Opt. Express **16**(26), 22126–22128 (2008).
11. K. M. Wang, H. Hu, F. Chen, F. Lu, B. R. Shi, D. Y. Shen, Y. G. Liu, J. Y. Wang, and Q. M. Lu, "Refractive index profiles in $YCa_4O(BO_3)_3$ and Nd:$YCa_4O(BO_3)_3$ waveguides created by MeV He ions," Nucl. Instrum. Methods Phys. Res. B **191**(1-4), 789–793 (2002).
12. A. Rodenas and A. K. Kar, "High-contrast step-index waveguides in borate nonlinear laser crystals by 3D laser writing," Opt. Express **19**(18), 17820–17833 (2011).
13. Y. Y. Ren, N. N. Dong, Y. C. Jia, L. L. Pang, Z. G. Wang, Q. M. Lu, and F. Chen, "Efficient laser emissions at 1.06 μm of swift heavy ion irradiated Nd:YCOB waveguides," Opt. Lett. **36**(23), 4521–4523 (2011).
14. Y. Y. Ren, Y. C. Jia, N. N. Dong, L. L. Pang, Z. G. Wang, Q. M. Lu, and F. Chen, "Guided-wave second harmonics in Nd:YCOB optical waveguides for integrated green lasers," Opt. Lett. **37**(2), 244–246 (2012).
15. A. G. Okhrimchuk, A. V. Shestakov, I. Khrushchev, and J. Mitchell, "Depressed cladding, buried waveguide laser formed in a YAG:Nd^{3+} crystal by femtosecond laser writing," Opt. Lett. **30**(17), 2248–2250 (2005).
16. N. N. Dong, F. Chen, and J. R. Vázquez de Aldana, "Efficient second harmonic generation by birefringent phase matching in femtosecond laser inscribed KTP cladding waveguides," Phys. Status Solidi: RRL **6**(7), 306–308 (2012).
17. Y. Jia, J. R. V. Aldana, C. Romero, Y. Ren, Q. Lu, and F. Chen, "Femtosecond-laser-inscribed BiB_3O_6 nonlinear cladding waveguide for second-harmonic generation," Appl. Phys. Express **5**(7), 072701 (2012).
18. H. Liu, Y. Jia, F. Chen, and J. R. Vázquez de Aldana, "Continuous wave laser operation in Nd:GGG depressed tubular cladding waveguides produced by inscription of femtosecond laser pulses," Opt. Mater. Express **3**(2), 278–283 (2013).

#187167 - $15.00 USD Received 18 Mar 2013; revised 29 Apr 2013; accepted 29 Apr 2013; published 3 May 2013

19. N. N. Dong, J. Martínez de Mendivil, E. Cantelar, G. Lifante, J. Vázquez de Aldana, G. A. Torchia, F. Chen, and D. Jaque, "Self-frequency-doubling of ultrafast laser inscribed neodymium doped yttrium aluminum borate waveguides," Appl. Phys. Lett. **98**(18), 181103 (2011).
20. M. Fujimura, T. Kodama, T. Suhara, and H. Nishihara, "Quasi-phase-matched self-frequency-doubling waveguide laser in Nd:$LiNbO_3$," IEEE Photon. Technol. Lett. **12**(11), 1513–1515 (2000).
21. Q. He, M. P. De Micheli, D. B. Ostrowsky, E. Lallier, J. P. Pocholle, M. Papuchon, F. Armani, D. Delacourt, C. Grezes-Besset, and E. Pelletier, "Self-frequency-doubled high Δn proton exchange Nd:$LiNbO_3$ waveguide laser," Opt. Commun. **89**(1), 54–58 (1992).

1. Introduction

The frequency doubling offers a platform for the wavelength extending and enlarges the family of available laser sources. In the conventional configuration of extracavity second harmonic generation (SHG), the nonlinear crystals are located out of the laser oscillating cavities [1,2], which results in long length of the whole systems. Modern photonics requires compact geometries in chip-scale circuit. A possible solution to realize integrated frequency converter is to employ composite crystals by bonding the active laser medium and the nonlinear material together [3]. Unfortunately, the benefits of simplification are often mitigated by its poor thermal stability and manufacturing difficulty. Self-frequency doubled (SFD) laser is an alternative solution, which is achieved by using the nonlinear gain crystals which combine both laser gain and nonlinearity into a single crystal. A SFD laser features lower reflection, absorption, and scattering losses which is appealing from a device point of view [4]. The Nd:$YAl_3(BO_3)_4$ (Nd:YCOB) crystal possesses large nonlinear coefficients, high emission cross section and high damage threshold, making it one of the most famous SFD crystals. However, its application and development are hindered from some problems, such as difficult growth and poor optical properties. Our research of SFD laser was focused on Nd:YCOB crystal due to its excellent features. Firstly, YCOB matrix allows high doping concentration of Nd^{3+} ions without obvious quenching of luminescence. The fluorescence lifetime at 1060 nm of Nd:YCOB (10%) was reported to be 96 μs. Secondly, Nd:YCOB crystal has high optical gain at 1.06 μm and a broader absorption band which matches well the emission wavelength of Ti:Sapphire laser. Furthermore, it shows high optical damage threshold at 1.06 μm (>1 GW/cm^2) and a nonlinear coefficient comparable with Nd:$YAl_3(BO_3)_4$ (1.1 pm/V) [5,6]. Nd:YCOB crystals with high quality have been produced with different methods and efficient self-frequency generation has been realized [4,7].

Optical waveguides, which allow confinement of the light in small volumes [8,9] provide further integration for the SFD system. In addition, many of the optical effects in the waveguides can be enhanced by the high intra-cavity light energy, which, for instance, enables lasing oscillation and nonlinear response at lower powers [10]. Up to now, planar and channel waveguides in Nd:YCOB have been reported, however, without demonstrating any lasing and SFD properties [11,12]. Nd:YCOB waveguide has been realized by Ar ion irradiation with planar morphology, which, although achieved waveguide laser emission, is not excellent for the development of three dimensional (3D) active waveguide circuits [13,14] More recently, depressed cladding waveguides fabricated by the ultrafast laser inscription (ULI), which were first reported in Nd:YAG [15], have attracted increasing attention. Its success lies in i) 3D wave-guiding structures which can be deeply embedded inside the sample without modifying the materials on the surface, ii) flexibility in shape and size, which could lead to high coupling efficiency between input mode and guiding mode, and iii) unique ability of propagating both transverse polarizations, meeting the requirement of birefringent phase matching for nonlinear frequency conversion [16,17].

In this work, we demonstrate the near-infrared and visible laser generations in the Nd:YCOB depresses cladding waveguides fabricated by using ULI.

2. Experiments

The Nd:YCOB (doped by 10 at.% Nd^{3+} ions) crystal was cut with a size of 2 × 5 × 8mm^3. For the realization of near infrared fundamental wave (1.06 μm) to green laser (0.53 μm)

#187167 - $15.00 USD Received 18 Mar 2013; revised 29 Apr 2013; accepted 29 Apr 2013; published 3 May 2013

conversion, the 5 mm dimension of the crystal was designed along the orientation of (θ, φ) = (150.3°, 0°) to satisfy the birefringence phase matching condition.

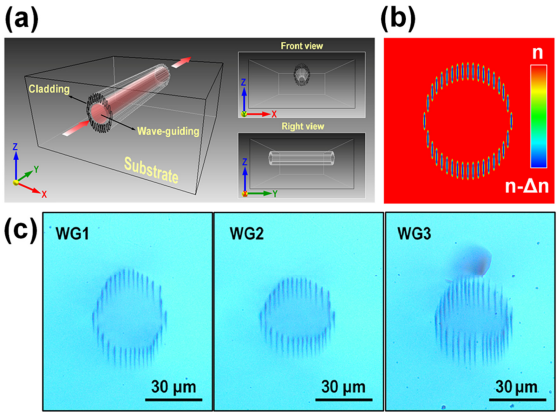

Fig. 1. (a) The schematic diagram of a cladding waveguide. The insets show the front and right views of the waveguide. (b) Refractive index profile of one cladding structure. (c) Depressed cladding structures fabricated in nonlinear Nd:YCOB crystal (end view).

Figure 1(a) shows the perspective diagram of a transparent substrate with a cladding waveguide embedded beneath the top surface (along *y*-axis in this figure), the front and right views of which are depicted in the insets of Fig. 1(a). Such a structure generally has a cladding with reduced refractive index and an unmodified core region, which can be illustrated with Fig. 1(b). In order to fabricate such compact and flexible structures, a Ti:Sapphire laser system (Spitfire, Spectra Physics, USA) was used as laser source, delivering 120 fs pulses with 1 kHz repetition rate. The central wavelength was 795 nm. The pulse energy was controlled by a calibrated neutral density filter and a set of half-wave plates together with a linear polarizer. The prepared Nd:YCOB was mounted to a computer controlled stage which can translate the sample in *x*-*y*-*z* direction with a high spatial resolution of 0.1 μm. The ultrafast laser pulses were focused through a microscope objective (NA = 0.65) into the substrate beneath one of the 5 × 8 mm^2 surfaces. While the sample was scanned through the laser focus along its 5-mm axis, the properties of the material in the focal area or its vicinity were modified and the waveguides were produced. The parameters eventually utilized to fabricate the desired structures are selected through a series of writing tests by compromising the large enough modification in the laser tracks and minimum cracks in the substrate. Once the irradiation parameters were selected, the scanning procedures were repeated in the same direction at different depths so as to form a tubular cladding. In this work, we fixed the scan speed (500 μm/s) and lateral separation between adjacent scans (3 μm) to write three structures with different pulse energies, which were 0.21 μJ for WG1, 0.42 μJ for WG2, and further increased to 0.84 μJ for WG3. The central depths of the structures were around 250 μm below the sample surface. The microscope image of the end view of each waveguide is presented in Fig. 1(c). The three structures were designed to have circular section with the same diameter of 30 μm. However, with the increasing of writing energies, the cross section of each track is longitudinally longer and the core area is further compressed in vertical direction. Nonetheless, as can be observed clearly, the materials in the tracks of all three structures are appropriately modified without damaging the core regions (which are expected to be the wave-guiding areas), revealing that the excellent properties of Nd:YCOB crystal are fairly well preserved in these areas. The refractive index reductions in the cladding areas have the order of 10^{-3}, which could be estimated by measuring the NA of the waveguides.

#187167 - $15.00 USD Received 18 Mar 2013; revised 29 Apr 2013; accepted 29 Apr 2013; published 3 May 2013

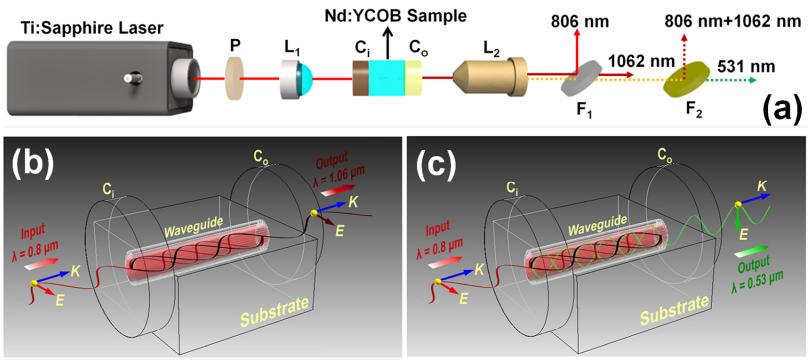

Fig. 2. (a) The schematic of the end-face coupling system, (b) and (c) illustrate the oscillation cavity for cladding waveguide lasing and self-frequency-doubling, respectively.

The experiments for waveguide lasing and SFD were implemented with an end-face coupling system, as illustrated in Fig. 2(a). A cw Ti:Sapphire laser (Coherent MBR 110) was utilized as pump source, the polarization of which was controlled by a half-wave plate. The pump beam with Gaussian spatial distribution was coupled into the waveguides with a convex lens (f = 50.8 mm), which give a diffraction limited pump spot size of about 35 μm ($1/e^2$ intensity diameter) at the focus, ensuring high overlap efficiency between the pumping mode and the wave-guiding mode. The output beam was collected by a 20 × microscope objective. The waveguide laser oscillation cavity employs a typical Fabry-Perot configuration where the sample was butt-coupled with two dielectric coupler mirrors (C_i and C_o), as clearly schematized in Figs. 2(b) and 2(c). The TE polarized pump light with a wavelength of 0.8 μm was coupled into the waveguides to excite a near infrared laser (1.06 μm), which play a role as fundamental wave for SFD. For near-infrared waveguide laser oscillation, the input mirror C_i provides high transmission at around 808 nm and high reflectivity at around 1064 nm, while the output coupler C_o has a transmittance of 5% at lasing wavelength. After being separated from the residual pump through a dichroic mirror, the laser emission from the waveguide was detected. The SFD of waveguide laser was realized with similar oscillation cavity, changing the input coupler to the one with high transmission at pumping wavelength and high reflectivity at fundamental laser and green laser wavelength. In this case, the output coupler was designed to have a reflectivity of ~99% at the fundamental wavelength and a high transmittance (~70% in our work) at around 532 nm. The output beam was also found to be a mixing of residual pumping light, fundamental wave as well as SFD radiation. Thus, a few filters were used to separate the SFD green lasers from the mixed output beam.

3. Results and discussion

The normalized spectra of pump light, fundamental wave and SFD laser are depicted in Fig. 3. The pump wavelength used in this work is 806 nm, where the best output powers for near infrared and green laser are achieved due to the strongest absorption of pumping power. As can be seen, the emission lines of fundamental wave and SFD green laser are peaked at 1062 nm and 531 nm, respectively, with the FWHM of (1.3 ± 0.1) nm. The laser emissions at 1062 nm were found to keep the same polarizing orientation (TE) with the pump laser, while the visible radiation were oscillating with transverse magnetic (TM) polarization, corresponding to TE^{ω} to $TM^{2\omega}$ frequency conversions, which are also illustrated in Figs. 2(b) and 2(c).

Figure 4 contains the experimental results for Nd:YCOB cladding waveguide lasing characterizations. Figure 4(a) demonstrates the corresponding lasing modes (TE polarized) emitted from WG1, WG2 and WG3, which show very distinct boundaries, suggesting that these waveguides are capable of propagating the near-infrared laser beams. The laser output power versus absorbed pump power is presented in Fig. 4(b). It has been found that the propagation losses of depressed cladding waveguides decrease with increasing core diameter [18] and the circular structure has high overlap efficiency between the pump and laser beams.

#187167 - $15.00 USD Received 18 Mar 2013; revised 29 Apr 2013; accepted 29 Apr 2013; published 3 May 2013

Therefore, WG1 shows best lasing performance with the lowest lasing threshold of 12.8 mW and highest slope efficiency of 55%. The maximum output power of 25 mW at 58 mW absorbed pump power was achieved, leading to an optical-to-optical conversion efficiency of 43%. WG3 gives a threshold for laser oscillation of 14.7 mW and slope efficiency of 48%. In contrast, for WG2, the lasing threshold raise to 17.1 mW and the slope efficiency reduced to 41%. The highest laser power generated from WG2 and WG3 are 14 mW and 20 mW, when the absorbed pump powers are 50 mW and 56 mW, respectively, corresponding to relatively lower optical conversion efficiencies of 28% and 36%. When compared with the Ar ion irradiated planar waveguide [13], it can be found that the slope efficiency of cladding waveguides is lower, which could be because 3D structures have higher propagation losses than the 2D one. However, the lasing thresholds obtained from cladding structures are much lower than that of the planar one due to their smaller effective areas.

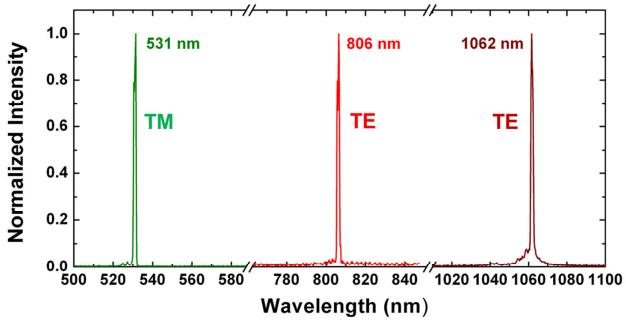

Fig. 3. Normalized spatial intensity distribution of the pump laser, the laser emission (fundamental wave in SFD) and the green laser.

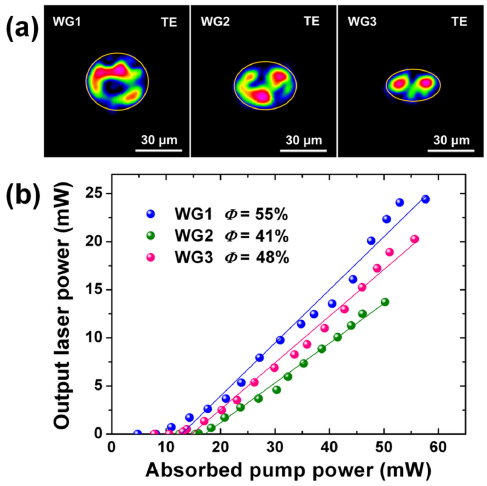

Fig. 4. Lasing performances of cladding waveguides in Nd:YCOB. (a) Near field intensity distributions of waveguide lasers at 1062 nm. The yellow circles are the boundaries of the guiding areas. (b) Experimental results of output near-infrared laser power as a function of absorbed pump power for WG1, WG2, and WG3.

The green radiation generated by SFD in the waveguide could be observed very clearly by naked eye, as displayed in Fig. 5(a), which is a photograph of the top-view of the laser cavity taken within a dark background. Figure 5(b) demonstrates the near field intensity distributions of green lasers generated from three cladding waveguides. It could be found from Fig. 4(a) and Fig. 5(b) that the measured transmission modes for both TE polarized waveguide laser at 1062 nm and TM polarized 531 nm SFD green laser are nearly circular for WG1, slight elliptic for WG2 and even oval-shaped for WG3, fitting very well with the cross section of

#187167 - $15.00 USD Received 18 Mar 2013; revised 29 Apr 2013; accepted 29 Apr 2013; published 3 May 2013

each waveguide. Among three waveguides, WG3 has least mode number due to the lower guiding region. Figure 5(c) plots the green laser power versus absorbed pumping power. It turned out as expected that the best performance was procured from WG1 with the maximum SFD output power up to 100 μW under the absorbed pump power of 72 mW. The highest green laser powers generated from WG2 and WG3 are 64 μW and 80 μW, when the absorbed pumping powers at 806 nm are 62.7 mW and 69.5 mW, respectively. Compared with the previous works on the SFD waveguide laser [14,19–21], the green laser powers achieved from these cladding structures are significantly larger. As a matter of fact, approximately 30 μW green laser radiation was obtained from a swift Ar^{8+} ion irradiated Nd:YCOB planner waveguide and double-line channel waveguides in Nd:YAB crystal [14,19]. Although not having as high power levels as those obtained from Nd:YCOB bulk crystal [4,7], the cladding waveguide laser SFD systems are more advantageous for low pumping power due to the highly compact oscillation, which leads to high intra-cavity intensity. In this work, the frequency conversion started at rather low absorbed pump power, less than 5 mW for all three waveguides. The better lasing and SFD performance can be expected by fabricating circular cladding waveguides with single transmission mode and low propagation losses.

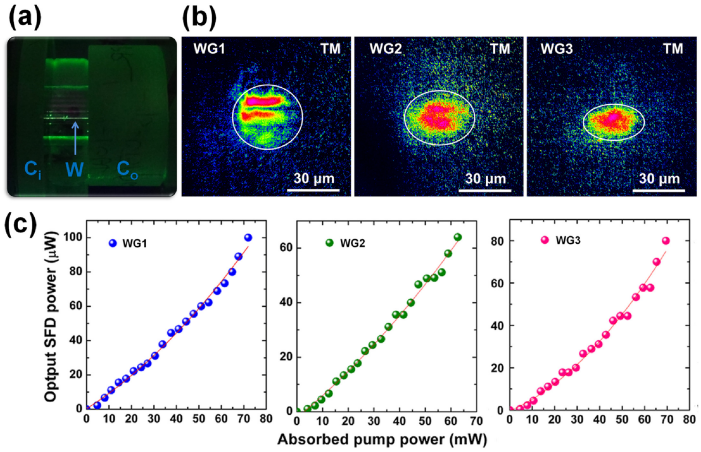

Fig. 5. (a) Photograph of the Fabry-Perot cavity employed for waveguide laser self-frequency-doubling experiments. W represents the green laser generation in the waveguide, which can be seen by naked eyes. (b) Mode distributions of green lasers generated from WG1, WG2 and WG3 (c) Output power of green laser obtained by SFD from WG1, WG2, and WG3.

4. Summary

We demonstrated cladding waveguides produced by ultrafast laser inscription in Nd:YCOB crystal. Efficient waveguide lasers at 1062 nm and guided SFD green lasers at 531 nm were realized in the waveguides, which provide us with compact, flexible and robust near-infrared and green laser sources.

Acknowledgments

This work was supported by the National Natural Science Foundation of China (No. 11274203), the Spanish Ministerio de Ciencia e Innovación (Projects CSD2007-00013 and FIS2009-09522), and Junta de Castilla y León (Project SA086A12-2).